THE JOURNAL OF PHYSICAL CHEMISTRY B

ARTICLE

pubs.acs.org/JPCB

Divalent Metal Cation Speciation and Binding to Surface-Bound Oligonucleotide Single Strands Studied by Second Harmonic Generation

Joseph G. Holland, David S. Jordan, and Franz M. Geiger*

Department of Chemistry, Northwestern University, 2145 Sheridan Road, Evanston, Illinois 60208, United States

Supporting Information

ABSTRACT: The binding of Sr(II), Ca(II), Mg(II), Ba(II), Mn(II), Zn(II), and Cd(II) to silica/water interfaces functionalized with $A_{15}T_6$ oligonucleotides was quantified at pH 7 and 10 mM NaCl using the Eisenthal $\chi^{(3)}$ technique. The binding free energies range from −31.1(6) kJ/mol for Ba(II) to −33.8(4) kJ/mol for Ca(II). The ion densities were found to range from 2(1) ions/strand for Zn(II) to 11(1) ions/strand for Cd(II). Additionally, we quantified Mg(II) binding in the presence of varying background electrolyte concentrations which showed that the binding free energies changed in a linear fashion from −39.3(8) to −27(1) kJ/mol over the electrolyte concentration range of 1−80 mM, respectively. An adsorption free energy versus interfacial potential analysis allowed us to elucidate the speciation of the bound Mg(II) ions and to identify three possible binding pathways. Our findings suggest that Mg(II) binds as a fully hydrated divalent cation, most likely displacing DNA-bound Na ions. These measurements will serve as a benchmark for computer simulations of divalent metal cation/DNA interactions for geochemical and biosensing applications.

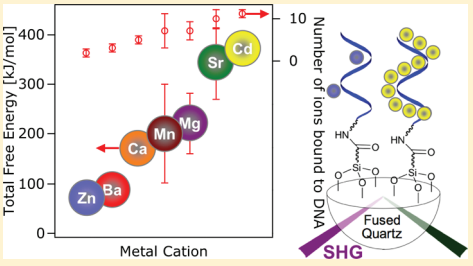

INTRODUCTION

The interaction of metal cations with short sequences of oligonucleotides is important in biosensor technologies and biodiagnostics[1−4] as well as DNA stabilization and replication.[5−10] Specific and nonspecific interactions are of interest in all of these areas of research, particularly for library screening methods such as the Systematic Evolution of Ligands by Exponential Enrichment (SELEX)[11,12] process yielding sequences with high overall binding affinity to specific targets.[13−25] While the library screening processes are effective for identifying oligonucleotide sequences, they can only identify the best hit from the library components. A more versatile and predictive approach would be to combine library screening with fundamental molecular insight into the quantification of specific and nonspecific target−oligonucleotide interactions. Given the immobilization of oligonucleotide capture strands at surfaces in many biosensors, such fundamental studies should ideally be carried out at interfaces. Here, we provide this insight for a number of metal cations interacting with one particular oligonucleotide sequence at pH 7 and controlled screening electrolyte concentration.

Given that metal ions are often the targets of aptamers or are indirectly involved in biosensing systems,[21,26−29] we focus here on the common divalent metal cations Sr(II), Ca(II), Mg(II), Ba(II), Mn(II), Zn(II), and Cd(II). Experimental techniques such as X-ray spectroscopy, NMR, circular dichroism, Raman, and IR have been used to study the binding of such metal ions[30−52] to DNA in the bulk. These studies collectively show that, on average, DNA interactions with transition metals are stronger than those with the alkaline earth metals. We study the metal−nucleotide interactions at interfacial environments because many biosensor readout and signal transduction processes rely on surface immobilization of the capture probes.[2,17,25,53−55] While at first glance one would expect surface specific results to be similar to those in bulk, due to the fact that interfacial processes often differ greatly from those in bulk solution,[2,3,56,57] it is desirable to directly study ion interactions with surface-bound DNA in a surface specific manner. Because labels can interfere with the system under investigation,[58] it is also desirable to apply highly sensitive label-free methods[26,59−65] for obtaining quantitative data about fundamental interfacial processes involving DNA.

Here, we choose second harmonic generation (SHG), a nondestructive, surface-specific, and label-free optical technique, which has proven successful in studying DNA at interfaces.[66−70] Following an overview of the thermodynamic and electrostatic results obtained for the various metal cations surveyed here, we further examine the interfacial speciation of Mg(II) because of its ubiquitous role in biology.[71−74] While the interaction of Mg(II) with DNA has been characterized in bulk solution by X-ray spectroscopy,[40−43] NMR,[44−46,75] IR,[47,48] Raman,[32,33] UV spectroscopy,[48,76] circular dichroism,[35,49,77] and computational studies,[78−80] which indicate that a fully hydrated Mg^{2+} ion interacts with deoxynucleotides through hydrogen bonding via an outer-sphere mechanism,[42,44,49,81] little is known about Mg(II) interactions with DNA-functionalized interfaces. Specifically, the

Received: March 28, 2011
Revised: May 24, 2011
Published: May 25, 2011

charge state of the Mg(II) ion bound to DNA at an interface is currently not known. We bridge this knowledge gap by taking advantage of free energy relationships in the electric double layer (EDL). The expectation is then that this work will serve as a surface-specific analogue to the existing body of bulk studies of the interaction of divalent metal cations with oligo- and polynucleotides and will serve as a benchmark for corresponding computational studies.

Background Theory. Second harmonic generation (SHG) is a nonlinear optical technique that is forbidden in centrosymmetric media within the electric dipole approximation.[82−84] Since this process is symmetry forbidden, the SH response originates from the interfacial region between two bulk phases, where a break in symmetry occurs. As we have shown previously, SHG is well-suited for studying the interaction of metal cations with silica/water interfaces functionalized with single-stranded DNA (ssDNA).[69] The experiments described in this work utilize a nonresonant variation of SHG called the Eisenthal $\chi^{(3)}$ technique. Akin to an "optical voltmeter", the $\chi^{(3)}$ technique utilizes the dependence of the second harmonic signal on the interfacial potential set up by a charged surface.[85] At pH 7, the ssDNA-silica/water interface is negatively charged due to the presence of the phosphate backbone of the DNA. These charges produce a static electric field, and thus a potential is generated at the interface. The total second-order polarization ($P_{2\omega}$) of the charged interface can be described as follows:

$$P_{2\omega} = \chi^{(2)} E_\omega E_\omega + \chi^{(3)} E_\omega E_\omega \Phi_0 \quad (1)$$

In this equation, $\chi^{(2)}$ and $\chi^{(3)}$ are the second- and third-order susceptibilities of the interface, E_ω is the incident electric field (set to be constant in these experiments), and Φ_0 is the interfacial potential. We have assumed a phase of zero between the second and third order susceptibility terms which has been demonstrated by Hayes et al. to be appropriate for modeling adsorption of alkaline earth metals at similar interfaces.[86] Thus, for constant input power, eq 1 can be simplified as follows:

$$\sqrt{E_{SHG}} = I_{SHG} \propto P_{2\omega} = A + B\Phi_0 \quad (2)$$

Equation 2 illustrates that the square root of the measured second harmonic signal intensity (I_{SHG}) is equal to the SHG electric field (E_{SHG}), which is proportional to the interfacial potential (Φ_0). On a molecular scale, the SHG response can be attributed to the presence of aligned water dipoles. We note that results from Campen et al. suggest that the hydrogen bonding strength of water, near the lipid DPPC surface in the presence of double-stranded DNA having about 48 thousand base pairs (i.e., not oligonucleotides), is not remarkably different in the presence and absence of Ca^{2+}.[87] This important finding supports the notion that the water dipoles that are aligned in the presence of the electrostatic potential studied here are passive reporters of the interfacial electrostatics as opposed to active participants in it (at least over the 100 fs pulse length produced by the laser systems).

Equation 2 is insensitive to changes in A and B that are relevant in this work, as shown in previously published sensitivity analyses.[69] Thus, eq 2 shows that changes in the interfacial potential can be monitored by tracking the intensity of the SH signal. Specifically, we expect that the negatively charged surface is screened by the positively charged metal ions when a divalent metal ion binds to the surface-tethered DNA. The resulting decrease in the interfacial potential should decrease the SH signal intensity, while the opposite is expected if the divalent metal dissociates from the surface-tethered DNA. Thermodynamic data are extracted from SHG results by expressing the interfacial potential (Φ_0) with an appropriately chosen model for the electric double layer (EDL) (eq 3),[88−91] such as the Gouy−Chapman model:[88−91]

$$\Phi_0 = \frac{2kT}{ze} \sinh^{-1}\left(\sigma\sqrt{\frac{\pi}{2\varepsilon kTC_{elec}}}\right) \quad (3)$$

The Gouy−Chapman model was chosen over other surface complexation models, such as the triple layer model, because it provides reasonable fits to the adsorption data without overparameterization.[91] The Gouy−Chapman model is also applicable to the interfacial potential range covered in these experiments.[89,91] Although the Gouy−Chapman equation is ideal for modeling the interfacial potential for symmetric electrolytes, we use it here as a first-order approximation for the case of a mixed electrolyte system.[86,92] In eq 3, and for all subsequent equations, constants k, T, and e have their usual definitions, C is the electrolyte concentration, z is the value of the charge of the screening electrolyte, and ε is the dielectric constant for water at 25 °C. As pioneered by Eisenthal and co-workers,[88,93] the following analyte-dependent expression was used to describe the surface charge density (σ) in the Gouy−Chapman equation (eq 4):

$$\sigma = \sigma_0 + \sigma_m\left(\frac{K_{obs}[M]}{1 + K_{obs}[M]}\right) \quad (4)$$

In eq 4, σ_0 is the experimentally determined initial surface charge density (C/m^2) of the DNA-functionalized surface in the absence of any metal, and σ_m is the maximum surface charge density (C/m^2) due to metal binding at saturation coverage. The value of σ_0 that was used for these experiments is −0.016 C/m^2, which was obtained from our previous work on the relationship between single-strand length and surface charge density.[66] It should be noted this σ_0 value is for single stranded 20-mers and would be expected to change upon switching to double-stranded oligonucleotides. Conversely, the value of σ_m is normally a positive number because the adsorption of positively charged species results in charge cancellation of the negatively charged surface sites. To scale the surface charge density by the divalent metal surface coverage, σ_m was multiplied by the Langmuir adsorption isotherm, which contains the observed binding constant, K_{obs}, and the bulk concentration of divalent metal, [M]. Equation 5 is the final fitting equation obtained by substituting eqs 3 and 4 into eq 2:[88,92−95]

$$E_{SHG} = A + B\prime\sinh^{-1}\left[\left(\sigma_0 + \sigma_m\left(\frac{K_{obs}[M]}{1 + K_{obs}[M]}\right)\right) \times \frac{30.19\ M^{-1/2}m^2C^{-2}}{\sqrt{C_{elec}}}\right] \quad (5)$$

Here, the numerical value of 30.19 is associated with the units of $M^{1/2}\,m^2/C^2$. Equation 5 was used to fit all the SHG adsorption isotherms to obtain both σ_m and K_{obs}, and from K_{obs} the Gibbs free energy of metal binding, ΔG_{bind}. For surface adsorption events that occur within the EDL, the binding free energy includes an electrostatic (i.e., Coulombic) term, and a chemical term involving non-Coulombic interactions such as hydrogen bonding, dipole−dipole interactions, and so forth. Thus,

the ΔG_{bind} for the binding between Mg(II) and surface-bound ssDNA can be defined as:

$$\Delta G_{bind} = \Delta G_{elect} + \Delta G_{chem} \quad (6)$$

In this equation, we further define the ΔG_{elect} as the work required to bring the positively charged Mg^{2+} ion into contact with the negatively charged ssDNA functionalized interface. Thus, eq 6 can be expressed as follows:

$$\Delta G_{bind} = F\Delta Z\Phi_0 + \Delta G_{chem} \quad (7)$$

In this equation, F is Faraday's constant, ΔZ is the change in charge of the surface species (in this case, the binding site of ssDNA) upon binding, and Φ_0 is determined for a given background electrolyte concentration by using the Gouy−Chapman equation (eq 3). Equation 7 illustrates that there is a linear relationship between the total binding free energy (ΔG_{bind}) and interfacial potential.[85,95,96] The slope of this line reveals the ΔZ parameter which was used to determine the charge state of the DNA-bound Mg(II) ions, as well as to elucidate probable binding pathways.

EXPERIMENTAL SECTION

A. Surface Functionalization and Materials. In all of the SHG experiments described herein, the substrates used were fused silica hemispheres (ISP Optics). The cleaning and preparation of these hemispheres has been previously reported.[95] The 21-mer oligonucleotide (Integrated DNA Technologies) used in this work was of the following sequence: $A_{15}T_6$: 5′-AAA AAA AAA AAA AAA TTT TTT/3AmMO/-3′. The strands were covalently attached to fused silica surfaces, previously functionalized with an *N*-hydroxysuccinimide linker, which reacts with the /3AmMO/-3′ modification, as described in our previous work.[66,67,69] Aqueous solutions were prepared using Millipore water and adjusted for pH by the addition of dilute HCl (E.M.D., ACS grade) and NaOH (Sigma-Aldrich, 99.99%). The pH 7 was used for convenience of comparison to other work. The aqueous solutions of the various metals were prepared by using $MgCl_2(H_2O)_6$ (Sigma-Aldrich, 99.99%), $MnCl_2(H_2O)_4$ (Sigma-Aldrich, 99.99%), $SrCl_2(H_2O)_6$ (Sigma-Aldrich, 99%), $BaCl_2(H_2O)_2$ (Sigma-Aldrich, 99%), $ZnCl_2$ (Sigma-Aldrich, 99.999%), $CaCl_2(H_2O)_2$ (Sigma-Aldrich, 99%), $CdCl_2$ (Allied Chemical, 99%), and NaCl (VWR, 99%). A Thermo Fisher pH meter was calibrated daily, and all metal concentrations were quantified using inductively coupled plasma atomic emission spectroscopy (ICP-AES, Varian). The laser and flow system used in all of the SHG experiments have been described previously.[92,94,97,98]

B. Adsorption/Desorption, "On/Off" Traces. Using our experimental flow setup, $\chi^{(3)}$ adsorption/desorption (on/off) traces were collected following our group's previously reported procedure for studying metal ion binding to solid−water interfaces.[92,94−99] The setup for the flow system consisted of two pumps and two reservoirs. While collecting the intensity of the SH signal (I_{SHG}), the background solution of NaCl (ranging from 1 to 80 mM) was flowed for several minutes to equilibrate the system. Once a stable background was reached, the flow from the first reservoir was stopped, and the flow from the second reservoir (containing both the same concentration of background NaCl plus a given concentration of the divalent metal) was started. The I_{SHG} was collected until the signal intensity reached a steady state following the expected drop in the signal level resultant from metal binding and lowering the interfacial potential. The time period in which divalent metal was flowing through the system constituted the "on" portion of the experiment. The "off" was achieved by once again flowing the NaCl solution from the first reservoir, and flushing the system of adsorbed divalent metal ions, until the I_{SHG} returned to the background level. This process was repeated with increasing concentrations of Mg^{2+} until the system reached binding saturation. All adsorption isotherms were recorded in at least duplicate.

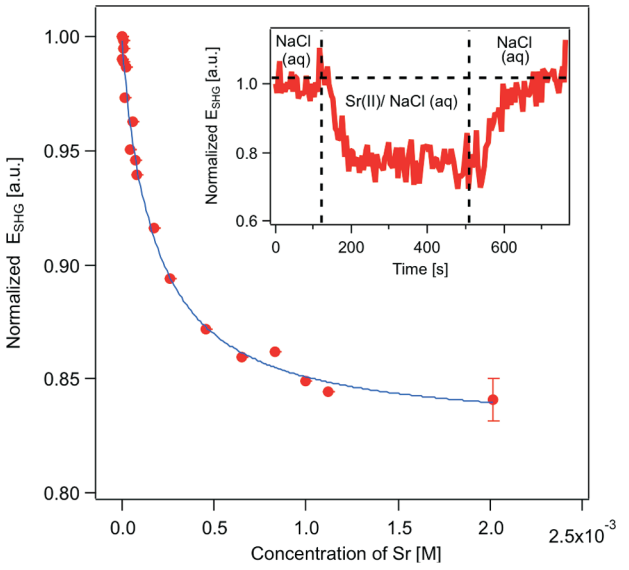

Figure 1. Adsorption isotherm for Sr(II) at the $A_{15}T_6$-functionalized fused silica/water interface carried out at pH 7 and in the presence of 10 mM NaCl. Data were collected in duplicate. The solid line is the fit of the data using eq 5. Inset. SHG E-field as a function of time for a flow rate of 1 mL/s, illustrating the reversibility of binding for a bulk concentration of 4.6×10^{-4} M $SrCl_2$.

RESULTS AND DISCUSSION

A. Binding Reversibility and Adsorption Isotherms for Ca(II), Ba(II), Mg(II), Sr(II), Mn(II), Zn(II), and Cd(II). The example "on/off" trace in the inset of Figure 1 shows the decrease in the E_{SHG} in the presence of 4.6×10^{-4} M bulk $SrCl_2$, consistent with the $\chi^{(3)}$ effect. As Sr(II) is flowed past the ssDNA-functionalized interface, the Sr(II) binds to the ssDNA, which in turn decreases the interfacial potential and thus decreases the E_{SHG} (eq 5). As seen in the inset, flushing the Sr(II) from the ssDNA with a solution of solely the background electrolyte returns the E_{SHG} to baseline levels, indicating that at pH 7, Sr(II)/DNA binding is fully reversible. Binding reversibility was also observed for all of the other metals studied in this work.

Adsorption isotherms were constructed by plotting the decrease in the SHG E-field (E_{SHG}) as a function of bulk metal concentration (see Figure 1). For all of the isotherms presented in this study, the magnitude of the E_{SHG} for adsorbed metal was determined by taking the square root of the I_{SHG}, which was normalized to the square root of the baseline I_{SHG} from the background NaCl solution. An example isotherm is presented in Figure 1 and shows the binding of Sr(II) to $A_{15}T_6$, at pH 7, and 10 mM NaCl. As was expected from eq 2, as bulk Sr(II) concentrations are increased (thus decreasing Φ_0), the E_{SHG} decreases until saturation of the DNA by Sr(II) occurs. Control studies have verified that the decrease in E_{SHG} is not merely the result

dx.doi.org/10.1021/jp202884n |J. Phys. Chem. B 2011, 115, 8338–8345

Table 1. Binding Constants, Free Energies of Binding, Ion Density per ssDNA Strand, and Total Free Energy of Binding of Various Divalent Metals with the $A_{15}T_6$-Functionalized Fused Silica Interface at 10 mM NaCl, 298 K, and pH 7[a]

	Mg	Ca	Sr	Ba	Mn	Zn	Cd
K_{obs} [M^{-1}]	$6(1) \times 10^3$	$15(2) \times 10^3$	$14(3) \times 10^3$	$5(1) \times 10^3$	$11(4) \times 10^3$	$11(4) \times 10^3$	$14(2) \times 10^3$
ΔG_{bind}[kJ/mol]	−31.5(5)	−33.8(4)	−33.6(6)	−31.1(6)	−33(1)	−33(1)	−33.6(4)
ion density [M^{2+} ions/strand]	7(2)	5(1)	10(2)	3(1)	7(4)	2(1)	11(1)
ΔG_{total}[kJ/mol]	−220(60)	−170(30)	−340(70)	−90(30)	−200(100)	−70(30)	−370(30)

[a] Binding free energy values obtained after referencing the 55.5 molarity of water.

of increasing ionic strength but that it is due to specific binding of divalent metals to the interface.[94] The solid line in Figure 1 is the fit of eq 5 to the adsorption data. Similar adsorption isotherms and fits were performed for all other metal ions under investigation. From the fits of the isotherms, we obtained both the binding constant (K_{obs}) and the maximum bound metal surface charge density (σ_m), which in turn allowed us to calculate both the binding free energy (ΔG_{bind}) with reference to 55.5 M water[100] and the ion density per 21-mer of DNA. The ion density (number of M(II) ions bound per DNA strand) was calculated from σ_m (eq 5) and the previously measured ssDNA surface coverage (5×10^{11} strands/cm^2).[66] The total binding free energy (ΔG_{total}) was also calculated as the product of binding free energy and ion density per 21-mer. These results are summarized for Mg(II), Ca(II), Sr(II), Ba(II), Mn(II), Zn(II), and Cd(II) in Table 1. The ΔG_{bind} values range from −31.1(6) to −33.8(4) kJ/mol for Ba(II) to Ca(II), respectively. These values are on the order of one or two hydrogen bonds and consistent with the notion that the metals are binding as hydrated ions via mechanism dominated by hydrogen bonding interactions. This result is consistent with bulk studies that show a fully hydrated Mg^{2+} ion interacts with deoxynucleotides through hydrogen bonding via an outer-sphere mechanism.[42,44,49,81] The ion density values range from 2(1) to 11(1) ions/strand for Zn(II) to Cd(II), respectively. Interestingly, there does not appear to be a direct correlation between the ion density and ΔG_{bind}. When comparing trends in our surface-bound system to previously published bulk studies,[32,77] we found a great extent of similarity in these two parameters. As an example, Duguid et al. reported that the binding of transition metals to dsDNA in bulk solution is on average greater than that of the alkaline earths, with the notable exception of Ca(II).[32] This trend is also apparent for surface bound ssDNA, with Sr(II) being a notable exception as it exhibits a free energy of binding comparable to that of the transition metals.

In an attempt to elucidate possible explanations for the trend in binding energies, we plotted the ΔG_{bind} as well as ΔG_{total} against several thermodynamic and physical properties, such as the ionic radius, polarizability, enthalpy of hydration, and so forth (see Supporting Information). These comparisons did not produce any discernible trends, suggesting that sequence specificity may dominate.

B. Free Energy/Interfacial Potential Relationships for Mg(II) Binding to ssDNA. Following this overview of metal−oligonucleotide interactions at interfaces, we performed a SHG speciation analysis for one specific metal of particular importance to biology, namely, Mg(II). To gain an understanding of the interfacial magnesium speciation, it was necessary to determine binding free energies for a series of adsorption isotherms at varying NaCl background concentrations (and thus varying interfacial potentials). This type of study, which compares ΔG_{bind} versus Φ_0, has proven useful in determining interfacial speciation

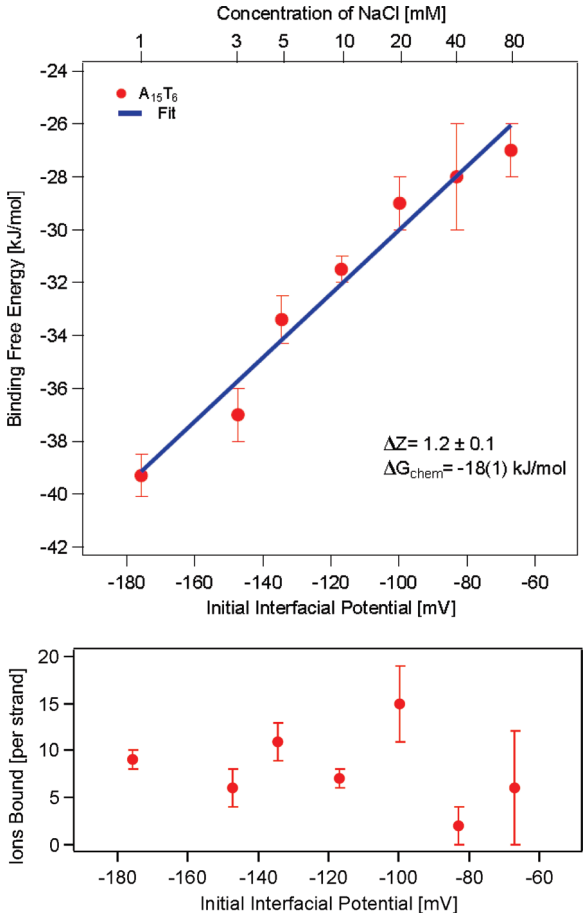

Figure 2. (A) Calculated free energy of binding as a function of electrolyte concentration (top axis) and initial interfacial potential (bottom axis) for Mg^{2+} at the $A_{15}T_6$ functionalized fused silica/water interface, at pH 7 and with NaCl. The solid line is the linear least-squares fit to the data. (B) The number of Mg(II) ions bound per strand as a function of initial interfacial potential is shown at pH 7.

of adsorbates and possible adsorption pathways to mineral oxide surfaces.[85,95,96] At background NaCl concentrations over 20 mM, there are larger errors in both the number of ions bound and the ΔG_{bind}. This can be attributed to decreased SHG signal intensity at salt concentrations above 40 mM.

Figure 2A shows the binding free energies (calculated from the $\chi^{(3)}$ adsorption isotherms) as a function of electrolyte concentration (top axis) and the corresponding initial interfacial potential (bottom axis). The interfacial potential was calculated at each given background concentration of NaCl using the Gouy−Chapman equation, with an initial surface charge density of −0.016 C/cm^2 for fused silica functionalized with a 21-mer of

dx.doi.org/10.1021/jp202884n |J. Phys. Chem. B 2011, 115, 8338–8345

Table 2. Binding Free Energies, Surface Charge Densities, Ion Number Densities, and Binding Constants for Mg^{2+} at the $A_{15}T_6$ Functionalized Fused Silica/Water Interface at 298 K and pH 7, as a Function of Background NaCl Concentration

	1 mM	3 mM	5 mM	10 mM	20 mM	40 mM	80 mM
ΔG_{bind}[kJ/mol]	−39.3(8)	−37(1)	−33.4(9)	−31.9(4)	−29(1)	−28(2)	−27(1)
σ_m [C/m^2]	0.015(1)	0.010(4)	0.017(3)	0.011(3)	0.024(6)	0.004(3)	0.01(1)
ion density [M^{2+} ions/strand]	9(1)	6(2)	11(2)	7(1)	15(4)	2(2)	6(6)
K_{obs} [M^{-1}]	14(4) × 10^4	5(2) × 10^4	1.3(4) × 10^4	0.6(1) × 10^4	0.26(9) × 10^4	0.17(8) × 10^4	0.08(3) × 10^4

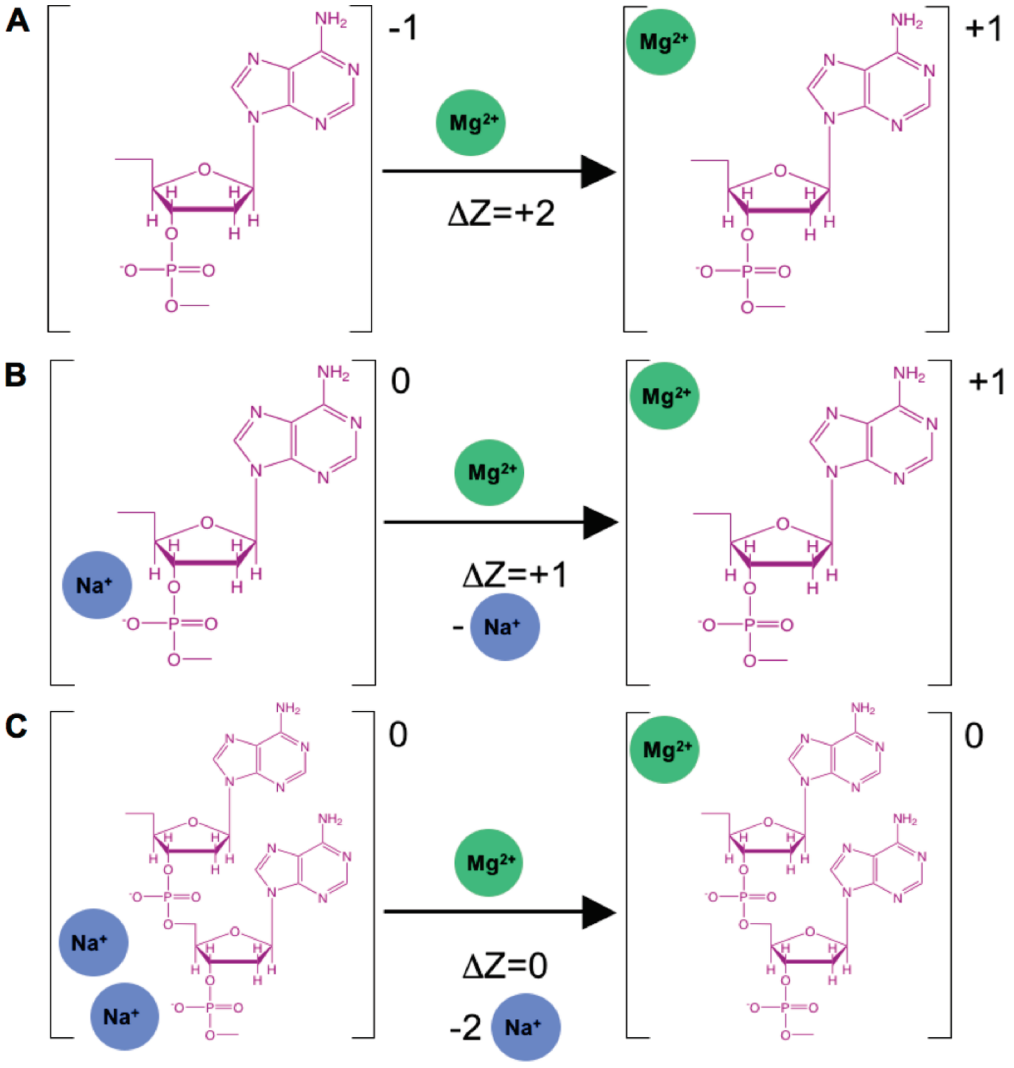

Figure 3. Proposed interaction pathways for Mg(II) binding to $A_{15}T_6$-functionalized fused silica/water interfaces. Chloride and other spectator ions are implicitly present, but not shown. Please see text for details.

ssDNA.[66] The experimentally determined binding free energies are listed in Table 2 and ranged from −39.3 to −27 kJ/mol for 1 to 80 mM NaCl, respectively. The errors associated with these binding free energies range from 0.5 to 2 kJ/mol. The ion density (ions bound per strand) is shown in Figure 2B and listed in Table 2. These results show that ion density is invariant with the background NaCl concentration. Thus, although the magnitude of binding free energy changes with interfacial potential, the amount of ions bound per strand does not. The average ion density for the range of NaCl concentrations examined is 8 ± 3. This data complement our previously published surface-specific work on Mg(II)/ssDNA binding[69] and agrees with computational, NMR, and X-ray diffraction (XRD) data that show Mg^{2+} ions bind to nucleotides in solution as the fully hydrated $Mg(H_2O)_6^{2+}$.[42,44,78,79,101]

As shown in Figure 2A, there is a linear relationship between the binding free energies and interfacial potential, which is to be expected based on eq 7. Subsequently, a linear least-squares analysis of the data shown in Figure 2 yields $F\Delta Z$ as the slope of the line and ΔG_{chem} as the y-intercept. The ΔG_{chem} for our system is −18(1) kJ/mol. The ΔZ value from the slope reveals the change in charge state of the binding site upon Mg(II)

binding to the surface-bound ssDNA, which we determine from our linear least-squares fit to be $+1.2 \pm 0.1$. The significance of this ΔZ value is discussed in the following section. Although there may be a slight curvature to the line, the slope does not flatten toward zero. This negates the possibility of a reduction in the Mg(II) charge state such as through ion pairing with Cl^-, which was observed for Sr(II) adsorption to the fused silica/water at higher background NaCl concentrations.[95]

C. Mg(II) Binding Pathways. The ΔZ result from our free energy versus potential analysis provides insight into the charge state of Mg adsorbates and allows us to draw conclusions about the plausible binding pathways for the Mg(II)/ssDNA interaction. Bulk studies have shown that Mg(II) binds predominantly to nucleotides via the negatively charged phosphate groups and the heteroatoms in the nitrogenous base.[81,101] Although SHG does not provide the Cartesian coordinates of atoms in the docking site and coordination atmosphere on the nucleotides, the ΔZ value we obtained from our analysis does allow us to propose binding pathways for hydrated Mg^{2+} to the nucleotide unit as a whole.[95,96] The ΔZ value of $+1.2$ confirms that the magnesium ion retains its overall $+2$ charge at the interface. If the effective charge of the magnesium adsorbates were to be lowered to $+1$ by ion pairing with screening electrolyte anions, the ΔZ value would have to be between zero and one.[95] Assuming an adsorbate speciation of Mg^{2+} and taking into account the ΔZ result, we propose three probable binding pathways for Mg^{2+} adsorption to surface-bound ssDNA (Figure 3). The first pathway (A) assumes that there are no Na^+ ions directly associated with the surface-bound ssDNA. After Mg^{2+} adsorption the charge on the nucleotide goes from -1 to $+1$, resulting in a ΔZ value for this scenario of $+2$. Similarly, a ΔZ value of $+2$ would be possible when two negatively charged (no Na^+ ions present) nucleotides were to be screened by one bound magnesium ion. Although possible, the range of interfacial potentials and screening of the nucleotides by sodium ions make this scenario unlikely. Next is pathway B, which involves one Na^+ ion associated with one nucleotide prior to adsorption. Upon magnesium binding, the sodium ion is displaced, resulting in a ΔZ value for this pathway of $+1$. Lastly, one multinucleotide binding pathway is proposed (C) in which two adjacent nucleotides each have one Na^+ ion associated with them. In this proposed pathway, one magnesium ion displaces two sodium ions, through multisite binding, to produce a ΔZ value of zero. Given the experimentally determined ΔZ value of $+1.2 \pm 0.1$, we propose that a combination of the three proposed pathways is operative under the condition of our experiments (Figure 3), where the availability of a Na^+ ion for phosphate screening scales with the background NaCl concentration. Though pathway C is likely to play a role at high electrolyte concentrations, the results indicate that pathways A ($\Delta Z = +2$) and B ($\Delta Z = +1$) dominate as reflected in the overall ΔZ of $+1.2$. These hypotheses are corroborated by bulk studies which show that DNA preferentially binds divalent ions over monovalent ions.[81,102] The ΔZ for $MgCl^+$ interacting with the nucleotides shown in scenarios A–C are $+1$, 0, and -1. This result suggests that $MgCl^+$ ion pairs are not the main constituents under the experimental conditions studied here but could be of minor importance.

CONCLUSION

In this work we have quantified, with a label-free method and directly at an aqueous/solid interface, how many and how strongly divalent transition and alkali earth metal ions interact with $A_{15}T_6$ 21-mers covalently linked to fused silica at the liquid–solid interface. The binding free energy values are indicative a hydrogen bond mediated outer-sphere binding mechanism, and ion densities were calculated to range from 2(1) to 11(1) ions/strand. In addition, we have utilized free energy relationships in the electrical double layer to model the observed free energy of binding as the sum of both an electrostatic term and a chemical term. Our results show Mg(II) binding to $A_{15}T_6$ has a ΔG_{chem} of $-18(1)$ kJ/mol and a ΔZ value of 1.2 ± 0.1, which leads us to conclude that magnesium binds to the nucleotide as $[Mg(H_2O)_6]^{2+}$ via a combination of three possible binding pathways that is dominated by an interaction that involves one Na^+ ion associated with one nucleotide prior to adsorption (pathway B in Figure 3). Future work will deconvolute the free energy of binding for the alkaline earth and transition metals into specific and nonspecific terms, similar to the work we have previously published for Mg(II).[69] Furthermore, we will examine the roles that nucleotide ordering and sequence play in binding, as well as the relationship between ion density and oligonucleotide length. Additionally, it would be beneficial to obtain ion densities and free energies of binding for double-stranded oligonucleotides, as one would expect the surface charge density and nucleobase accessibility to change significantly for these systems. We hope that this data will serve as a useful complement to aptamer studies involving surface bound oligonucleotides that interact either directly or indirectly with divalent metal cations.

ASSOCIATED CONTENT

Supporting Information. Individual adsorption isotherms for all metals studied and plots of free energy of binding versus various thermodynamic and physical properties. This material is available free of charge via the Internet at http://pubs.acs.org.

AUTHOR INFORMATION

Corresponding Author
*E-mail: geigerf@chem.northwestern.edu.

ACKNOWLEDGMENT

This work was supported by the Northwestern University Nanoscale Science and Engineering Center (NSEC) and the National Science Foundation Environmental Chemical Sciences program under Grant No. CHE-0950433. We also acknowledge the International Institute for Nanotechnology (IIN) at Northwestern University for capital equipment support and an Irving M. Klotz professorship to FMG. We acknowledge Spectra-Physics Lasers, a division of Newport Corporation, for equipment support. The ICP-AES analysis was completed at the Northwestern University Integrated Molecular Structure Education and Research Center (IMSERC).

REFERENCES

(1) Liu, J.; Lu, Y. *Chem. Rev.* **2009**, *109*, 1948.
(2) Cho, E. J.; Lee, J.-W.; Ellington, A. D. *Annu. Rev. Anal. Chem.* **2009**, *2*.
(3) Lee, J. S.; Han, M. S.; Mirkin, C. A. *Angew. Chem. Int. Ed.* **2007**, *46*, 4093.
(4) Kim, H.-S.; Jung, S.-H.; Kim, S.-H.; Suh, I.-B.; Kim, W. J.; Jung, J.-W.; Yuk, J. s.; Kim, Y.-M.; Ha, K.-S. *Proteomics* **2006**, *6*, 6426.

(5) Record, M. T., Jr. *Biopolymers* **1977**, *14*, 2137.
(6) Bleam, M. L.; Anderson, C. F.; Record, M. T., Jr. *Proc. Natl. Acad. Sci.* **1980**, *77*, 3085.
(7) Pelletier, H.; Sawaya, M. R.; Kumar, A.; Wilson, S. H.; Kraut, J. *Science* **1994**, *264*, 1891.
(8) Hartwig, A. *Mutat. Res./Fundam. Mol. Mech. Mutagenesis* **2001**, *475*, 113.
(9) Owczarzy, R.; Moreira, B. G.; You, Y.; Behlke, M. A.; Walder, J. A. *Biochemistry* **2008**, *47*, 5336.
(10) Yang, L.; Arora, K.; Beard, W. A.; Wilson, S. H.; Schlick, T. *J. Am. Chem. Soc.* **2004**, *126*, 8441.
(11) Tuerk, C.; Gold, L. *Science* **1990**, *249*, 505.
(12) Djordjevic, M. *Biomol. Eng.* **2007**, *24*, 179.
(13) Bunka, D. H. J.; Stockley, P. G. *Nat. Rev. Microbiol.* **2006**, *4*, 588.
(14) Mairal, T.; Cengiz Özalp, V.; Lozano Sánchez, P.; Mir, M.; Katakis, I.; O'Sullivan, C. *Anal. Bioanal. Chem.* **2008**, *390*, 989.
(15) Hermann, T.; Patel, D. J. *Science* **2000**, *287*, 820.
(16) Brody, E. N.; Willis, M. C.; Smith, J. D.; Jayasena, S.; Zichi, D.; Gold, L. *Mol. Diagn.* **1999**, *4*, 381.
(17) Tombelli, S.; Minunni, M.; Mascini, M. *Biosens. Bioelectron.* **2005**, *20*, 2424.
(18) Wang, J. *Nucleic Acids Res.* **2000**, *28*, 3011.
(19) Ng, J. H.; Ilag, L. L.; El-Gewely, M. R. Biochips beyond DNA: technologies and applications. In *Biotechnology Annual Review*; Elsevier: New York, 2003; Vol. 9, p 1.
(20) Elbaz, J.; Shlyahovsky, B.; Li, D.; Willner, I. *ChemBioChem* **2008**, *9*, 232.
(21) Wernette, D. P.; Swearingen, C. B.; Cropek, D. M.; Lu, Y.; Sweedler, J. V.; Bohn, P. W. *Analyst (Cambridge, U.K.)* **2006**, *131*, 41.
(22) Feng, K.; Kang, Y.; Zhao, J.-J.; Liu, Y.-L.; Jiang, J.-H.; Shen G.-L.; Yu, R.-Q. *Anal. Biochem.* **2008**, *378*, 38.
(23) Osborne, S. E.; Matsumura, I.; Ellington, A. D. *Curr. Opin. Chem. Biol.* **1997**, *1*, 5.
(24) Dick, L. W.; McGown, L. B. *Anal. Chem.* **2004**, *76*, 3037.
(25) Wan, Y.; Kim, Y.-t.; Li, N.; Cho, S. K.; Bachoo, R.; Ellington, A. D.; Iqbal, S. M. *Cancer Res.* **2010**, *70*, 9371.
(26) Smirnov, I. V.; Kotch, F. W.; Pickering, I. J.; Davis, J. T.; Shafer, R. H. *Biochemistry* **2002**, *41*, 12133.
(27) Li, L.; Li, B.; Qi, Y.; Jin, Y. *Anal. Bioanal. Chem.* **2009**, *393*, 2051.
(28) Cherian, S.; Gupta, R. K.; Mullin, B. C.; Thundat, T. *Biosens. Bioelectron.* **2003**, *19*, 411.
(29) Xue, X.; Wang, F.; Liu, X. *J. Am. Chem. Soc.* **2008**, *130*, 3244.
(30) Thorpe, J. H.; Gale, B. C.; Teixeira, S. C. M.; Cardin, C. J. *J. Mol. Biol.* **2003**, *327*, 97.
(31) Tereshko, V.; Wilds, C. J.; Minasov, G.; Prakash, T. P.; Maier, M. A.; Howard, A.; Wawrzak, Z.; Manoharan, M.; Egli, M. *Nucleic Acids Res.* **2001**, *29*, 1208.
(32) Duguid, J.; Bloomfield, V. A.; Benevides, J.; Thomas, G. J., Jr. *Biophys. J.* **1993**, *65*, 1916.
(33) Duguid, J. G.; Bloomfield, V. A.; Benevides, J. M.; Thomas, G. J., Jr. *Biophys. J.* **1995**, *69*, 2623.
(34) Gao, Y.-G.; Sriram, M.; Wang, A. H.-J. *Nucleic Acids Res.* **1993**, *21*, 4093.
(35) Clement, R. M.; Sturm, J.; Daune, M. P. *Biopolymers* **1973**, *12*, 405.
(36) Granot, J.; Kearns, D. R. *Biopolymers* **1982**, *21*, 203.
(37) Kennedy, S. D.; Bryant, R. G. *Biophys. J.* **1986**, *50*, 669.
(38) Braunlin, W. H.; Nordenskiöld, L.; Drakenberg, T. *Biopolymers* **1989**, *28*, 1339.
(39) Langlais, M.; Tajmir-Riahi, H. A.; Savoie, R. *Biopolymers* **1990**, *30*, 743.
(40) Chiu, T. K.; Dickerson, R. E. *J. Mol. Biol.* **2000**, *301*, 915.
(41) Gessner, R. V.; Quigley, G. J.; Wang, A. H. J.; Van der Marel, G. A.; Van Boom, J. H.; Rich, A. *Biochemistry* **1985**, *24*, 237.
(42) Subirana, J. A.; Soler-Lopez, M. *Annu. Rev. Biophys. Biomol. Struct.* **2003**, *32*, 27.
(43) Gessner, R. V.; Frederick, C. A.; Quigley, G. J.; Rich, A.; Wang, A. H. *J. Biol. Chem.* **1989**, *264*, 7921.
(44) Cowan, J. A.; Huang, H. W.; Hsu, L. Y. *J. Inorg. Biochem.* **1993**, *52*, 121.
(45) Wright, L. A.; Lerner, L. E. *Biopolymers* **1994**, *34*, 691.
(46) Rose, D. M.; Polnaszek, C. F.; Bryant, R. G. *Biopolymers* **1982**, *21*, 653.
(47) Hackl, E. V.; Kornilova, S. V.; Kapinos, L. E.; Andrushchenko, V. V.; Galkin, V. L.; Grigoriev, D. N.; Blagoi, Y. P. *J. Mol. Struct.* **1997**, *408*−*409*, 229.
(48) Ahmad, R.; Arakawa, H.; Tajmir-Riahi, H. A. *Biophys. J.* **2003**, *84*, 2460.
(49) Kankia, B. I. *Biophys. Chem.* **2003**, *104*, 643.
(50) Soler-López, M.; Malinina, L.; Tereshko, V.; Zarytova, V.; Subirana, J. *J. Biol. Inorg. Chem.* **2002**, *7*, 533.
(51) Zimmer, C.; Luck, G.; Triebel, H. *Biopolymers* **1974**, *13*, 425.
(52) Waalkes, M. P.; Poirier, L. A. *Toxicol. Appl. Pharmacol.* **1984**, *75*, 539.
(53) Lautner, G.; Balogh, Z. f.; Bardóczy, V.; Mészáros, T.; GyurcsAnyi, R. A. b. E. *Analyst (Cambridge, U.K.)* **2010**, *135*, 918.
(54) D'Orazio, P. *Clin. Chim. Acta* **2003**, *334*, 41.
(55) Wang, J.; Lv, R.; Xu, J.; Xu, D.; Chen, H. *Anal. Bioanal. Chem.* **2008**, *390*, 1059.
(56) Somorjai, G. A. *Introduction to Surface Chemistry and Catalysis*; John Wiley & Sons, Inc.: New York, 1994.
(57) Brown, G. E.; et al. *Chem. Rev.* **1999**, *99*, 77.
(58) Liu, J.; Conboy, J. C. *Biophys. J.* **2005**, *89*, 2522.
(59) Wurpel, G. W. H.; Sovago, M.; Bonn, M. *J. Am. Chem. Soc.* **2007**, *129*, 8420.
(60) Chen, Y.; Nguyen, A.; Niu, L.; Corn, R. M. *Langmuir* **2009**, *25*, 5054.
(61) Barhoumi, A.; Zhang, D.; Halas, N. J. *J. Am. Chem. Soc.* **2008**, *130*, 14040.
(62) Moses, S.; Brewer, S. H.; Lowe, L. B.; Lappi, S. E.; Gilvey, L. B. G.; Sauthier, M.; Tenent, R. C.; Feldheim, D. L.; Franzen, S. *Langmuir* **2004**, *20*, 11134.
(63) Libera, J. A.; Cheng, H.; Olvera de la Cruz, M.; Bedzyk, M. J. *J. Phys. Chem. B* **2005**, *109*, 23001.
(64) Mourougou-Candoni, N.; Naud, C.; Thibaudau, F. *Langmuir* **2003**, *19*, 682.
(65) Georgiadis, R.; Peterlinz, K. P.; Peterson, A. W. *J. Am. Chem. Soc.* **2000**, *122*, 3166.
(66) Boman, F. C.; Gibbs-Davis, J. M.; Heckman, L. M.; Stepp, B. R.; Nguyen, S. T.; Geiger, F. M. *J. Am. Chem. Soc.* **2009**, *131*, 844.
(67) Boman, F. C.; Musorrafiti, M. J.; Gibbs, J. M.; Stepp, B. R.; Salazar, A. M.; Nguyen, S. T.; Geiger, F. M. *J. Am. Chem. Soc.* **2005**, *127*, 15368.
(68) Stokes, G. Y.; Gibbs-Davis, J. M.; Boman, F. C.; Stepp, B. R.; Condie, A. G.; Nguyen, S. T.; Geiger, F. M. *J. Am. Chem. Soc.* **2007**, *129*, 7492.
(69) Holland, J. G.; Malin, J. N.; Jordan, D. S.; Geiger, F. M. *J. Am. Chem. Soc.* **2011**, *133*, 2567.
(70) Walter, S. R.; Geiger, F. M. *J. Phys. Chem. Lett.* **2009**, *1*, 9.
(71) Maguire, M. E.; Cowan, J. A. *BioMetals* **2002**, *15*, 203.
(72) Elin, R. J. *Am. J. Clin. Pathol.* **1994**, *102*, 616.
(73) Theophanides, T.; Anastassopoulou, J. *Magnesium: current status and new developments, theoretical, biological and medical aspects*; Kluwer Academic Publishers: The Netherlands, 1997.
(74) Wolf, F. I.; Cittadini, A. *Mol. Aspects Med.* **2003**, *24*, 3.
(75) Rose, D. M.; Bleam, M. L.; Record, M. T.; Bryant, R. G. *Proc. Natl. Acad. Sci.* **1980**, *77*, 6289.
(76) Sissoëff, I.; Grisvard, J.; Guillé, E. *Prog. Biophys. Mol. Biol.* **1978**, *31*, 165.
(77) Eichhorn, G. L.; Shin, Y. A. *J. Am. Chem. Soc.* **1968**, *90*, 7323.
(78) Solt, I.; Simon, I.; Csaszar, A. G.; Fuxreiter, M. *J. Phys. Chem. B* **2007**, *111*, 6272.
(79) Misra, V. K.; Draper, D. E. *J. Mol. Biol.* **1999**, *294*, 1135.
(80) MacKerell, A. D. *J. Phys. Chem. B* **1997**, *101*, 646.
(81) Anastassopoulou, J.; Theophanides, T. *Crit. Rev. Oncol./Hematol.* **2002**, *42*, 79.

(82) Eisenthal, K. B. *Chem. Rev.* **1996**, *96*, 1343.
(83) Eisenthal, K. B. *Chem. Rev.* **2006**, *106*, 1462.
(84) Boyd, R. W. *Nonlinear Optics*, 2nd ed.; Academic Press: New York, 2003.
(85) Hayes, P. L.; Chen, E. H.; Achtyl, J. L.; Geiger, F. M. *J. Phys. Chem. A* **2009**, *113*, 4269.
(86) Hayes, P. L.; Malin, J. N.; Jordan, D. S.; Geiger, F. M. *Chem. Phys. Lett.* **2010**, *499*, 183.
(87) Campen, R. K.; Ngo, T. T.; Sovago, M.; Ruysschaert, J.-M.; Bonn, M. *J. Am. Chem. Soc.* **2010**, *132*, 8037.
(88) Yan, E. C. Y.; Liu, Y.; Eisenthal, K. B. *J. Phys. Chem. B* **1998**, *102*, 6331.
(89) Langmuir, D. *Aqueous Environmental Geochemistry*; Prentice Hall: Upper Saddle River, NJ, 1997.
(90) Morel, F. M. M.; Hering, J. G. *Principles and Applications of Aquatic Chemistry*; John Wiley & Sons, Inc.: New York, 1993.
(91) Stumm, W.; Morgan, J. J. *Aquatic Chemistry*, 3rd ed.; John Wiley & Sons, Inc.: New York, 1996.
(92) Hayes, P. L.; Malin, J. N.; Konek, C. T.; Geiger, F. M. *J. Phys. Chem. A* **2008**, *112*, 660.
(93) Salafsky, J. S.; Eisenthal, K. B. *J. Phys. Chem. B* **2000**, *104*, 7752.
(94) Malin, J. N.; Hayes, P. L.; Geiger, F. M. *J. Phys. Chem. C* **2009**, *113*, 2041.
(95) Malin, J. N.; Holland, J. G.; Geiger, F. M. *J. Phys. Chem. C* **2009**, *113*, 17795.
(96) Malin, J. N.; Geiger, F. M. *J. Phys. Chem. A* **2010**, *114*, 1797.
(97) Hayes, P. L.; Gibbs-Davis, J. M.; Musorrafiti, M. J.; Mifflin, A. L.; Scheidt, K. A.; Geiger, F. M. *J. Phys. Chem. C* **2007**, *111*, 8796.
(98) Mifflin, A. L.; Musorrafiti, M. J.; Konek, C. T.; Geiger, F. M. *J. Phys. Chem. B* **2005**, *109*, 24386.
(99) Al-Abadleh, H. A.; Voges, A. B.; Bertin, P. A.; Nguyen; Geiger, F. M. *J. Am. Chem. Soc.* **2004**, *126*, 11126.
(100) Williamson, A. W. *Physical Chemistry of Surfaces*, 5th ed.; John Wiley & Sons: New York, 1990.
(101) Tajmir-Riari, H. A.; Theophanides, T. *Can. J. Chem.* **1985**, *63*, 2065.
(102) McFail-Isom, L.; Sines, C. C.; Williams, L. D. *Curr. Opin. Struct. Biol.* **1999**, *9*, 298.